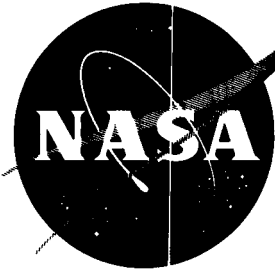


39

N63-14025  
code-1



# TECHNICAL NOTE

D-1275

LAUNCH DEFLECTOR DESIGN CRITERIA  
AND THEIR APPLICATION  
TO THE SATURN C-1 DEFLECTOR

By R. L. Evans and O. L. Sparks

George C. Marshall Space Flight Center  
Huntsville, Alabama

**CASE FILE  
COPY**

NATIONAL AERONAUTICS AND SPACE ADMINISTRATION  
WASHINGTON

March 1963

554044  
42P

103 12

NATIONAL AERONAUTICS AND SPACE ADMINISTRATION

---

TECHNICAL NOTE D-1275

---

LAUNCH DEFLECTOR DESIGN CRITERIA  
AND THEIR APPLICATION  
TO THE SATURN C-1 DEFLECTOR

By

R. L. Evans and O. L. Sparks

SUMMARY

14025

Theoretical considerations pertinent to the successful design of dry launch deflectors for super boosters are presented. Deflector configurations of many types, together with the particular configuration used in the launching of the C-1 Saturn booster, are described.

It is concluded that the dry deflector can be successfully used to launch super boosters. In particular, it is predicted that the Saturn deflector may be used unlimitedly without the necessity of extensive overhaul and repairs.

SECTION I. INTRODUCTION

The high thrust rocket engines used in present day missiles and space vehicles release large quantities of energy in the form of exhaust gases. These high temperature, supersonic velocity exhaust jets create serious hazards to personnel, structures, ground support equipment, and instrumentation at the launch sites. The continuing trend toward larger and higher thrust engines, with the concomitant increase in hazards, makes it essential that accurate methods be established for predicting and controlling the exhaust jets effects.

The quantity and distribution of the exhaust jet energy depend on several variable factors. The total energy available is determined by the type and amount of propellant used; the form and rate of energy release is controlled by the rocket engine design and the number of engines; and distribution of the energy in the area surrounding the launcher is controlled by the exhaust flame deflector design. Since the magnitude of the first two of these variables is determined by the vehicle design criteria to meet given mission requirements, the flame deflectors must

be designed for controlled deflection of a predetermined amount of energy at the launch site. In the following sections, various types of deflectors are discussed, and the general design criteria for an uncooled heat-sink type deflector are developed. These criteria are applicable to a broad range of thrust levels which should include the booster systems of space vehicles to be developed in the foreseeable future. Although theory has been developed and is of significant value in designing flame deflectors, it should not be construed that the theory provides all necessary design information. Rather, the theory must be supplemented with an extensive model test program.

The successful launching of the first Saturn space vehicle (C-1) provided additional verification of the design criteria developed for the uncooled flame deflector.

## SECTION II. ROCKET ENGINE EXHAUST ENERGY

The thrust developed by a rocket engine depends upon the propellant mass flow rate and the exhaust velocity. The exhaust velocities of most LOX/RP-1 engines currently being used are approximately equal. Typical velocity distribution patterns in free-flowing rocket engine exhausts at sea level, for engines rated at 80,000 and 150,000 lb thrust, are shown in FIGURES 1 and 2, respectively.

The axial velocity of the jet stream on the jet axis can be determined by the following empirical formulas: (Ref. 1)

The axial velocity of the center of the jet stream of the jet axis will remain unchanged until

$$X = \frac{D_o/2}{0.053} \quad (1)$$

where  $X$  = distance from nozzle discharge

$D_o$  = nozzle exit diameter

When the distance  $X$  is greater than the value given by this equation, the gas velocity on the axis decreases according to the following relation:

$$\log_{10} \frac{U_x}{U_o} \frac{X}{D_o} = 0.79 - 33 \frac{r^2}{X^2} \quad (2)$$

where  $U_x$  = axial velocity of gas on jet axis at X

$U_0$  = axial velocity of gas at nozzle exit

r = radius of gas jet penetration from axis into ambient air

For an underexpanded or overexpanded jet, the mixing and velocity dissipation will occur more rapidly than indicated by these equations.

The temperature distribution in the exhausts of the same two engines, shown in FIGURES 3 and 4, indicates a wider range of energy distribution for the larger engine. This is to be expected since much more energy is available in the larger engine.

The hazards created at the launch site by these high temperature, high velocity exhaust gases during the launching of a missile or space vehicle make it necessary to devise methods for control and dissipation of this energy. One method of accomplishing this is by the use of flame deflectors.

### SECTION III. DISSIPATION OF EXHAUST ENERGY

1. Flame Deflectors. Direct impingement and uncontrolled flow of rocket engine exhaust gases during a launching would create serious hazards to the launch vehicle and ground equipment due to spalling, melting of metallic objects, and dislodgment in the direct impingement area. A flame deflector is a mechanical device placed in the exhaust stream to prevent the blast from impinging directly on the launch pad and to channel the exhaust away from the launcher area to reduce or eliminate these hazards. Distribution of the exhaust is controlled by the type and design of the deflector. The exhaust may be channeled in one or two directions, or all around the launcher. In a cooled deflector, the coolant absorbs a large amount of heat from the exhaust, thus reducing the energy in the exhaust stream. An uncooled deflector absorbs only a small amount of the heat, and reduces the energy level of the exhaust jet very little.

When an exhaust jet impinges on a deflector, its velocity decreases while the temperature and pressure increase. The impingement angle determines the amount of velocity decrease. As the exhaust gases flow away from the deflector, the front of the blast compresses the atmosphere ahead of it, and this increase in pressure causes the gases to expand radially which reduces the gas pressure and transfers heat to the atmosphere, thereby reducing the exhaust temperature. This action continues until a state of equilibrium is reached with the surrounding atmosphere.

Since very few materials have the physical and mechanical properties required to withstand the high temperatures, pressures, and velocities of the exhaust jet, prevention of melting and erosion of the deflector material is a major problem. Erosion can be largely eliminated by maintaining the surface temperature below the melting point of the deflector surface material. Several methods of accomplishing this surface temperature control have been developed and the deflectors employed may be generally classified as "cooled" and "uncooled" types.

2. Cooled Deflectors. Water is used to cool the deflector to maintain the temperature of the deflector surface below the melting point of the material used. Several deflector designs of this type have been developed based on different methods of employing the water coolant. One method used is to introduce water into the exhaust stream through spray nozzles located upstream from the deflector to reduce the exhaust temperature and maintain the surface material below the melting point. Another method frequently used is to circulate water through a manifold beneath the deflector plate through which many small holes have been drilled. All, or a portion of, the water may be forced through these holes into impingement area to provide evaporation and film cooling of the deflector surface. Other variations of these methods have been employed to meet special requirements.

These methods are effective, but require a large water supply, a high capacity pumping and plumbing system, and extensive maintenance which result in high initial and operating costs. Therefore, this type of cooled deflector is impractical for use with tactical missiles and operational space vehicles. However, when long duration static firings are required, a water-cooled deflector is usually provided.

At static test sites, the cooled deflector provides an additional advantage by reducing the overall sound pressure level through reduction of the energy level in the exhaust stream. However, this advantage would be lost at a launch site at lift-off.

3. Uncooled Deflectors. Uncooled flame deflectors must rely on their physical properties to withstand the erosive action and high temperatures of the engine exhaust. They may be generally classified as the "heat-sink" or "ablation" type based on the characteristics method of heat transfer employed to control surface temperatures.

In a heat-sink type deflector, a material with high thermal conductivity is used to conduct the heat away from the surface rapidly enough to prevent melting. Theoretically, this type deflector will not lose surface material and should, therefore, have a long life. This type deflector was developed by the Army Ballistic Agency for use with the Redstone and Jupiter missiles, and was recently employed with complete success in launching the Saturn booster (C-1 vehicle).

An ablation type deflector is designed to take advantage of the erosive effect of the exhaust. The deflector base material is coated with an erodible material with a low thermal conductivity. As the surface material erodes under the action of the exhaust stream, heat is removed with the eroded particles which reduces the surface temperature and the amount of heat transferred to the base material. Periodic replacement of the erodible surface material is required, depending upon the thickness of the material used, the duration of each exposure, and the rate of erosion. In conclusion, it should be noted that many deflectors depend on the heat-sink principle and ablation material for their operation.

#### SECTION IV. UNCOOLED DEFLECTOR DESIGN CRITERIA

1. Heat Transfer. The major problems associated with the design of uncooled flame deflectors evolve from the high rate of heat transfer from the exhaust jet to the deflector surface and the limited heat transfer capabilities of the deflector materials which must remove this heat rapidly enough to prevent melting.

Although the exhaust gases flow over the deflector surface at high velocities, a film of stagnant gas forms next to the surface and acts as an insulator which reduces the rate of heat transfer to the surface material. The thickness of this stagnant film depends on such variables as bulk density, viscosity, thermal conductivity, specific heat of the exhaust gases, and the velocity of the gases parallel to the surface. The relationship of these variables and the local heat transfer coefficient may be expressed by the empirical equation for turbulent flow over a flat plate: (Ref. 2)

$$\frac{h_x X}{k} = 0.0296 \left( \frac{\rho V_x X}{\mu} \right)^{4/5} \left( \frac{C_p \mu}{k} \right)^{1/3} \quad (3)$$

- where
- $h_x$  = local heat transfer coefficient of the film
  - $X$  = distance downstream from the initial impingement point
  - $k$  = thermal conductivity of the gas
  - $\rho$  = bulk density of the gas
  - $V_x$  = gas velocity parallel to the surface
  - $\mu$  = gas viscosity
  - $C_p$  = specific heat of the gas

The coefficient of heat transfer of the film is also influenced by other considerations such as shock waves, impingement angle, and boundary layer.

2. Shock Waves. A shock wave is a planar discontinuity or boundary which is produced when a supersonic jet stream impinges on a surface. The shock wave may be normal to or at an angle to the direction of fluid flow, depending upon the position of the deflecting surface with relation to the direction of flow. Shock waves cause abrupt changes in the properties of the fluid flowing through the wave. The type of shock wave produced determines the extent of change in the fluid properties. Since the rate of heat transfer to the deflecting surface depends, to a large extent, on the downstream properties of the flowing fluid, it is evident that an analysis of shock waves to determine their influence on heat transfer rates is necessary in the design of any rocket engine flame deflector. Shock waves may be generally classified as normal and oblique, based on their position relative to the direction of fluid flow.

A normal shock is a discontinuity produced in a plane perpendicular to the direction of fluid flow. Fluid flowing through a normal shock undergoes a sudden rise in static pressure, density, enthalpy, and temperature, and a corresponding decrease in velocity and isentropic stagnation pressure. At certain upstream Mach numbers, the downstream static pressure and temperature can increase to almost combustion chamber values. In the case of normal shocks, it is possible to express the upstream and downstream properties of the fluid in terms of the upstream Mach number ( $M_e$ ) and the ratio of specific heats ( $\gamma$ ). These relations may be expressed by the following equations for flow through a normal shock where the subscripts e and 2 refer, respectively, to conditions upstream and downstream from the shock; (Ref. 3)

Exit Mach number ( $M_2$ ) (4)

$$M_2 = \frac{M_e^2 + \frac{2}{\gamma - 1}}{\frac{2\gamma}{\gamma - 1} M_e^2 - 1}$$

Static Pressure Ratio:

$$\frac{P_2}{P_e} = \frac{2\gamma}{\gamma + 1} M_e^2 - \frac{\gamma - 1}{\gamma + 1} \quad (5)$$

Temperature Ratio:

$$\frac{T_2}{T_e} = \frac{\left(1 + \frac{\gamma - 1}{2} M_e^2\right) \left(\frac{2\gamma}{\gamma - 1} M_e^2 - 1\right)}{\frac{(\gamma + 1)^2}{2(\gamma - 1)} M_e^2} \quad (6)$$

$\gamma$  = ratio of specific heats

An oblique shock wave is produced when a supersonic jet stream impinges on an inclined surface and is turned in a direction that causes interference in the flow of adjacent layers of the stream. FIGURE 5 illustrates the system geometry of such a condition where a supersonic jet with Mach number  $M_e$  impinges on a flat plate inclined at an angle  $\delta$  to the stream flow direction which results in an oblique shock wave being formed at an angle  $\sigma$  to the stream flow.

From the aerodynamic equations of continuity, the momentum and energy equations, and the system geometry, (FIGURE 6) the following equation is derived: (Ref. 2)

$$\frac{1}{M_e^2} = \sin^2 \sigma - \frac{\gamma + 1}{2} \frac{\sin \sigma \sin \delta}{\cos(\sigma - \delta)} \quad (7)$$

where  $M_e$  = free flow Mach number (upstream)

$\sigma$  = angle between flow direction and shock wave (shock angle)

$\gamma$  = ratio of specific heats

$\delta$  = angle between flow direction and impingement surface (impingement or deflection angle)

For a given upstream Mach number and specific heat ratio, this equation may be used to determine either  $\sigma$  or  $\delta$  by assuming a value of one and solving for the other.

A velocity vector diagram of the fluid flow in relation to an oblique shock wave is illustrated in FIGURE 6. The subscripts n and t indicate the velocity components which are normal to and parallel to the shock wave, respectively. Similarly, subscripts e and 2 denote the conditions upstream and downstream from the shock wave. An oblique shock wave acts as a normal shock wave to the component of the fluid stream that is normal to the oblique shock wave. Therefore, by assuming an infinite field of flow, and a value for angle  $\delta$ , an analysis can be made of the fluid properties downstream from an oblique shock wave.

For a given upstream Mach number and specific heat ratio, equation (7) can be used to determine the value of angle  $\sigma$  for the assumed value of angle  $\delta$ . Once these angles are determined, the downstream Mach number, pressure, and temperature can be determined by use of the normal shock



equations (4), (5), and (6) and the proper trigonometric relations. From FIGURE 6, the value of the velocity component normal to the shock ( $M_e \sin \sigma$ ) must be substituted for  $M_e$  in all three equations. Furthermore, since the value of  $M_2$  obtained from the use of equation (4) represents the normal component of the downstream Mach number ( $M_{2n}$ ), this value must be divided by  $\sin (\sigma - \delta)$  to obtain the Mach number of the downstream fluid which flows parallel to the surface of the inclined flat plate. Since temperature and pressure are scalar quantities, it is unnecessary to modify the downstream values determined by use of equations (5) and (6).

3. Impingement Angle. The angle formed by the flow direction of an impinging jet and the inclined upstream surface is generally referred to as the impingement angle. However, when the deflecting surface is a flat plate, it is sometimes referred to as the deflection angle, since the upstream and downstream angles formed at the point of impact are equal. For given upstream fluid properties, the impingement angle  $\delta$  determines the fluid properties downstream of the shock wave and the rate of heat transfer to the deflecting surface.

The inclination of the shock wave relative to the downstream deflector surface is determined by the difference between the shock angle  $\sigma$  and the impingement angle  $\delta$ . This relationship is shown in FIGURE 7 for a given upstream fluid condition which closely approaches those of the Saturn booster. It should be noted that the equation becomes indeterminate above certain values of  $\delta$  for each upstream fluid condition assumed. This critical angle  $\delta_c$  is the angle at which the shock wave separates from the deflecting surface and allows exhaust gases to flow up the plate, thus reducing the mass flow downstream. For the conditions assumed for FIGURE 7, the critical angle  $\delta_c$  is approximately 41 degrees. In practice, however, the viscosity of the exhaust stream fluid causes a certain amount of backflow to occur at any impingement angle. However, for angles above the critical values, the resulting backflow conditions are much more severe. The critical angle is not important when the exhaust impinges on the apex of a cone or pyramid-shaped deflector, or on the leading edge of a two-way deflector. However, it must be considered in the design of unidirectional flow deflectors and when the jet impinges on the sloped surface of a multidirectional deflector.

FIGURES 8, 9, and 10 show, respectively, the relation between the impingement angle and the downstream Mach number, static pressure, and temperature for an exhaust jet with specific upstream characteristics. In this instance, exhaust jet characteristics approximating those of the Saturn booster were employed.

As mentioned, the rate of heat transfer to the deflector is dependent upon the impingement angle. FIGURE 11 is an experimental curve determined from tests on a 5000-lb thrust rocket which shows that the heat transfer coefficient is a function of the sine of the impingement angle. (Ref. 4).

The impingement angle is also important in the determination of the forces acting on a deflector in the impingement area. Determination of these forces is discussed in 5 below.

4. Boundary Layer. When an exhaust stream flows over a deflecting surface, the velocity of the fluid particles adjacent to the surface is reduced to almost zero due to friction between the surface and the fluid. Similarly, each successive layer of fluid is affected to a decreasing extent until they finally reach mainstream velocity. These low velocity layers form a film or boundary layer on the deflector surface which acts as an insulator or thermal barrier to the passage of heat. The insulating effect of the boundary layer is a function of its thickness which is dependent on the properties of the fluid and nature of the flow over the surface.

The boundary layer thickness (which is the distance normal to the deflector surface) required for the fluid to reach mainstream velocity is a function of the velocity, density, and dynamic viscosity of the fluid, and the distance downstream from the point of initial impingement. The properties can be combined into the dimensionless Reynolds number as follows:

$$N_{re} = \frac{\rho V_x X}{\mu} \quad (8)$$

where

$N_{re}$  = Reynolds number

$\rho$  = density of exhaust fluid

$V_x$  = downstream velocity of exhaust

$X$  = distance downstream from initial impingement point

$\mu$  = dynamic viscosity of the fluid

Fluid flow over a surface may be described as laminar or turbulent. When the fluid layers next to the surface flow smoothly, even though they have different relative velocities, the condition is referred to as laminar flow. When the flow of the fluid layers is rough, and unpredictable eddies are formed, the condition is referred to as turbulent flow. Immediately after impingement, a boundary layer is formed on the deflecting surface. At the point of impingement, the thickness of the boundary layer is negligible and the coefficient of heat transfer is maximum. For a short distance downstream from the point of impingement, laminar flow occurs and boundary layer thickness increases which results in a decreasing heat transfer coefficient. Transition from laminar flow to

turbulent flow occurs at a point downstream from the initial impingement point; here, the boundary layer decreases in thickness and the heat transfer coefficient is again a maximum. This transition point is believed to be between Reynolds numbers of  $10^5$  and  $2 \times 10^6$ . FIGURE 12 shows the relation between the impingement angle  $\delta$  and the downstream distance to the transition point  $X$  for the two Reynolds number limits. Surface roughness or eroded particles in the exhaust stream can cause sufficient change in the Reynolds number to affect the location of the transition point, but such effects were not considered in determination of the two curves illustrated.

When a supersonic jet impinges on a flat plate at some angle  $\delta$ , a shock pattern is known to develop. FIGURE 13 shows the theoretical pattern developed, together with the variation of static pressure and the film heat transfer coefficient. Circled odd numbers indicate regions of low pressure, and circled even figures indicate regions of high pressure. The variation in the average heat transfer coefficient is also shown. It is to be noted that the greater the distance over which the heat transfer coefficient is averaged, the lower will be the value of the film coefficient. The greatest damage to the deflector will occur at the point of maximum coefficient. Even though the average coefficient may be low, burnout at a point may occur due to a high local film coefficient. This high local film coefficient may be attributed to disturbances in the boundary layer due to the formation of complex shock waves, changes in flow direction, and in the case of multiple jets, to the interaction of jet streams.

5. Forces. A study of the forces acting on a deflector under the impact of a supersonic jet stream shows a definite relationship between these forces and the jet impingement angles on a flat and curved plate. A diagram of the forces acting on a typical deflector surface is illustrated in FIGURE 14. From the force and angular relationships shown, certain pertinent equations can be derived if the following assumptions are made:

- a.  $\delta$  (impingement angle)  $< \delta_c$  (critical impingement angle for shock detachment), two dimensional flow.
- b. Total mass flow leaves both flat plate number 1 and curved plate number 2 as essentially parallel flow.
- c. No shock losses over the curved plate number 2, i. e., constant velocity over plate number 2.
- d. Inviscid flow.

Then, the horizontal and vertical forces acting on the flat plate number 1 are as follows:

$$F_{H_1} = \frac{F}{2} \sin (2 \delta_1) \quad (9)$$

$$F_{V_1} = F \sin^2 \delta_1 \quad (10)$$

where  $F = \text{jet force } (\frac{\text{mass flow rate} \times \text{velocity}}{g})$

$F_{H_1} = \text{horizontal component of force on plate number 1}$

$F_{V_1} = \text{vertical component of force on plate number 1}$

$\delta_1 = \text{impingement angle on plate number 1}$

These equations are applicable for any fluid jet of any configuration which impinges on an inclined flat plate, when the mass flow leaving the plate is parallel to the surface. Within the assumed limits of  $\delta_1$ , these relationships are for inviscid flow. FIGURE 15 shows the ratio  $F_{V_1}/F$  and the ratio  $F_{H_1}/F$  versus the impingement angle  $\delta_1$ , for a flat plate deflector (Section number 1). The scale imposed on the abscissa shows the relationship of the Mach number of an air jet ( $\gamma = 1.4$ ) to the deflector critical angle or shock detachment angle as determined from Equation (5). It shows that, as the jet Mach number increases, the value of the shock detachment angle  $\delta_c$  increases.

Since the net force acting on the curved plate section number 2 is equal to  $F \cos \delta_1$ , then the forces acting on the curved plate section number 2 shown in FIGURE 14 may be expressed by the following equations which are applicable to loss-free turning vanes with two-dimensional flow:

$$F_{N_2} = F \cos \delta_1 \sin \delta_2 = F \cos^2 \delta_1 \quad (11)$$

$$F_{T_2} = F \cos \delta_1 (1 - \cos \delta_2) = F \cos \delta_1 (1 - \sin \delta_1) \quad (12)$$

$$F_{H_2} = F_{N_2} \cos \delta_1 - F_{T_2} \sin \delta_1 = F \cos \delta_1 (1 - \sin \delta_1) \quad (13)$$

$$F_{V_2} = F_{T_2} \cos \delta_1 + F_{N_2} \sin \delta_1 = F \cos^2 \delta_1 \quad (14)$$

where  $F_{H_2} = \text{horizontal component of force on curved plate number 2}$

$F_{V_2}$  = vertical component of force on curved plate  
number 2

$F_{T_2}$  = tangential component of force on curved plate  
number 2

$F_{N_2}$  = normal component of force on curved plate number 2

The ratio  $F_{V_2}/F$  and the  $F_{H_2}/F$  versus the compliment of the impingement angle ( $\delta_2$ ) for the curved plate deflector section number 2 is shown on FIGURE 16.

6. Materials. Metals are the logical materials for conductive or heat-sink type deflectors. Any metal selected must be capable of conducting heat away from the deflector surface at a rate that will maintain the exposed surface at a temperature below its melting point. Several metals having high melting temperatures and thermal conductivities are also capable of withstanding high thermal and mechanical shocks. However, when all factors are considered, mild steel and copper appear to be the most suitable for deflectors. Copper has a much higher thermal conductivity than steel, but steel has a higher melting point. FIGURES 17 and 18 show, respectively, the calculated thickness of steel and copper required to maintain the surface temperature below the melting point in relation to impingement angle and exposure time. These illustrations show that the required thickness of steel is less than copper but the variation in thickness for different impingement angles is greater. As a result of various tests by Government agencies at Redstone Arsenal since 1951, it has been empirically determined that carbon steel is more suitable than copper for heat-sink type deflectors.

FIGURE 19 shows the relation between thickness of a mild steel deflection plate and the calculated time required to raise the surface temperature to approximately 90 percent of its melting temperatures. This figure is based upon the following information which closely approximates conditions of the Saturn booster and deflector configuration:

Heat Transfer Coefficient	$h = \text{Btu/hr ft}^2 \text{ } ^\circ\text{F}$
Impingement Angle	$\delta = 30^\circ$
Ratio of Specific Heats	$\gamma = 1.2$
Mach Number of Exhaust Jet	$M_e = 3.12$
Stagnation Temperature	$T_o = 6430^\circ\text{R}$
Static Temperature	$T_e = 3260^\circ\text{R}$
Recovery Temperature	$T_{\text{Recovery}} = 6254^\circ\text{R}$

From this graph it is apparent that the time required is directly related to metal thicknesses, up to a certain thickness, beyond which, thickness has no influence on the ability of the material to absorb heat. A material thickness of 1 inch was selected for the Saturn flame deflector.

## SECTION V. UNCOOLED FLAME DEFLECTOR CONFIGURATIONS

1. Typical Designs. The amount of heat transferred to a deflector is a function of the impingement angle and dwell time of the exhaust stream. As dwell time increases, smaller impingement angles are required to reduce the heat transfer rate. However, since smaller impingement angles increase the deflector height, and hence, the height of the launcher, it is desirable to employ the largest possible impingement angle. Any deflector design must be based on a compromise between these requirements. Several successful deflector designs with certain common features have been developed to meet the special requirements for different missiles and space vehicles.

With any type deflector, the greatest blast effects occur in the area of initial impingement, where the downstream flow direction is changed, and where a stagnant front is formed. To reduce boundary layer disturbances, deflectors should be designed so that the area of impingement is a flat surface and the area of the deflector which changes the downstream direction of fluid has a large radius of curvature. The entire surface of the deflector should be smooth and free from projections to reduce the formation of stagnant points and prevent local burnouts. The special features of a particular launcher and vehicle must also be considered, e.g., a multiengine booster might be oriented with respect to the deflector to have the exhausts of the engines ride one upon the other. Several typical deflector designs and the major characteristics of each are discussed in the following paragraphs.

a. Flat Plate. The simplest deflector configuration is a flat plate positioned in the vehicle exhaust stream so that the jet impinges normal to its surface. It is characterized by very high heat transfer rates which make it suitable only for vehicles having a short launcher dwell time and relatively low propellant mass flow rates. It should be noted that this type deflector precludes the placing of any ground support equipment in close proximity to the launcher, since severe damage may be incurred from the nondirected exhaust.

b. Dish-Shaped. Dish-shaped deflectors are also characterized by high heat transfer rates. Ground support equipment cannot be placed in the vicinity of the launcher due to the wide spreading of the exhaust jet. In addition, their geometry causes the exhaust stream to be reversed with the inherent possibility of damage to the booster vehicle tail section.

c. Unidirectional Deflector. The unidirectional or bucket type deflector consists of a curved section or an inclined straight section and curved section combination which directs the exhaust gases away from the launcher area. Local heat transfer rates tend to be high at the initial impingement point on the straight section and at the joining of the straight and curved sections (secondary impingement point).

d. Wedge-Shaped Deflector. The wedge-shaped deflector is the type used on Launch Complex 34 (LC 34) for the Saturn (C-1) firing and is formed by joining together two unidirectional deflectors. This type of deflector is particularly adaptable to multiengine booster vehicles, as the deflector height may be reduced to approximately one-half that of the unidirectional deflector height by having the engine exhausts impinging on both sides of the deflector. Care must be exercised to ensure that the engine exhausts do not impinge directly on the leading edge of the deflector, since high heat transfer rates would occur. When this condition cannot be avoided (five engines), provisions must be made to water-cool the leading edge or part of it. A reduction in the horizontal forces required to secure this type of deflector in place, as compared with the unidirectional type, is obtained since these forces may be balanced.

2. Saturn Flame Deflector. The deflector used for the C-1 firing is a culmination of the efforts of design engineers using the analytical approach already outlined, and the test engineers using model studies. Report No. MTP-M-TEST-61-14, 1:20 Scale Model Saturn Launch Deflector Studies, by C. P. Verschoore, presents a breakdown of the tests run on a scale model Saturn launcher deflector. It is interesting to note here that the average heat transfer coefficients for the model and full scale deflectors conform to the following relationship: (Ref. 2)

$$h_{x_{avg}} \text{ full scale} = \left( \frac{X \text{ Model}}{X \text{ full scale}} \right)^{0.2} h_{x_{avg}} \text{ model} \quad (15)$$

$h_{x_{avg}}$  = average heat transfer coefficient  
over some distance X downstream  
from the initial impingement point.

Since local heat transfer coefficients for model and prototype may be equal, and as shown by equation (15), the average heat transfer coefficient of the model is greater than the prototype. It is necessary to use water as a coolant for model tests.

FIGURE 20 shows the C-1 deflector configuration arrived at by the joint efforts of the design and test engineers. The flame pattern of the Saturn vehicle as it impinges on the deflector during holddown is shown on FIGURE 21. The recent firing of the Saturn booster was a verification of the approach taken by the proponents of the uncooled flame

deflector for launching of super boosters. FIGURE 22 is a photograph of the C-1 deflector after launching of the Saturn vehicle. As can be seen by comparing FIGURES 20 and 22, the deflector came through the C-1 firing literally unscathed, i.e., the deflector needs only to be repainted prior to reuse. Instead of the 8 to 10 firing use predicted, postfiring inspection indicates the deflector life may be practically unlimited.



**THRUST AT SEA LEVEL 80,000 LB**  
**NOZZLE AREA RATIO 25:1**  
**NOZZLE EXIT DIAMETER 46.1 INCH**  
**PROPELLANTS LOX & RP-1**  
**CHAMBER PRESSURE 659 PSIA**  
**NOZZLE EXIT PRESSURE 2.8 PSIA**

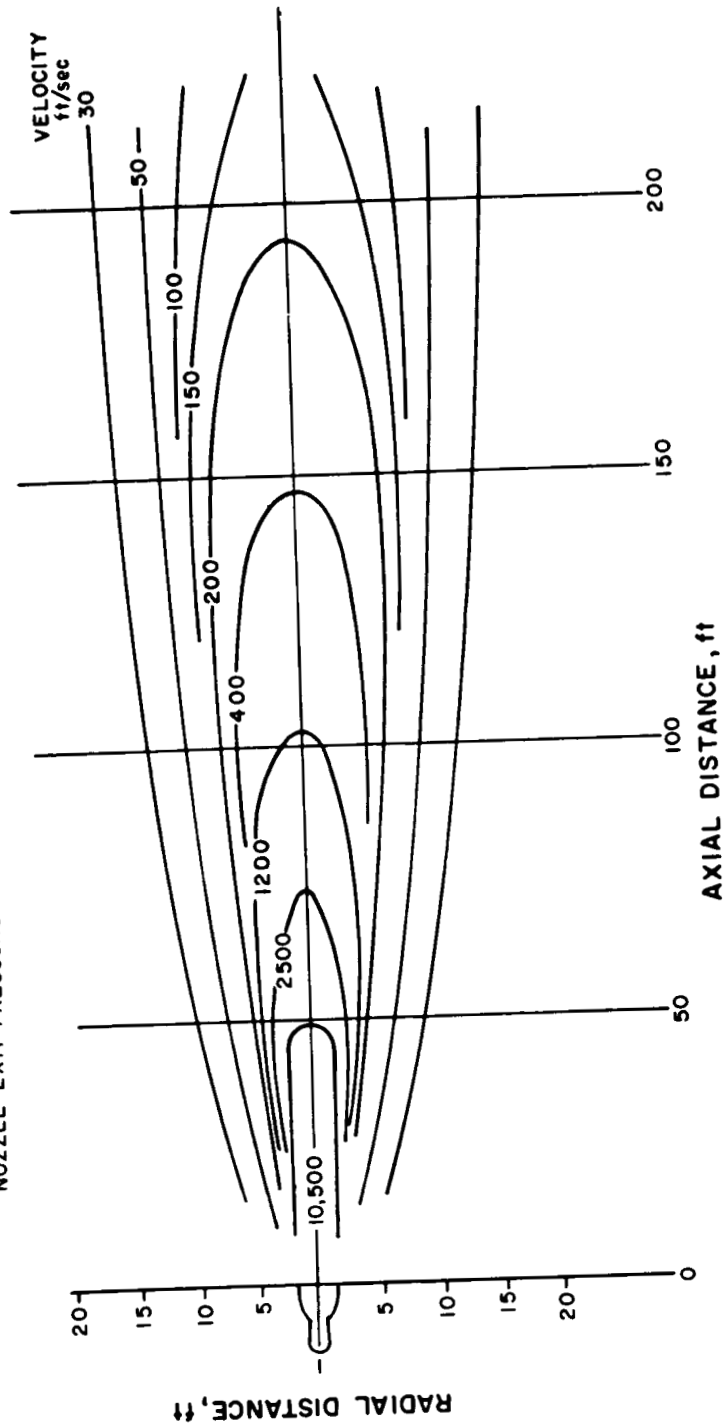


FIGURE 1. VELOCITY DISTRIBUTION IN EXHAUST AT SEA LEVEL OF AN 80,000-POUND  
 THRUST ROCKET ENGINE

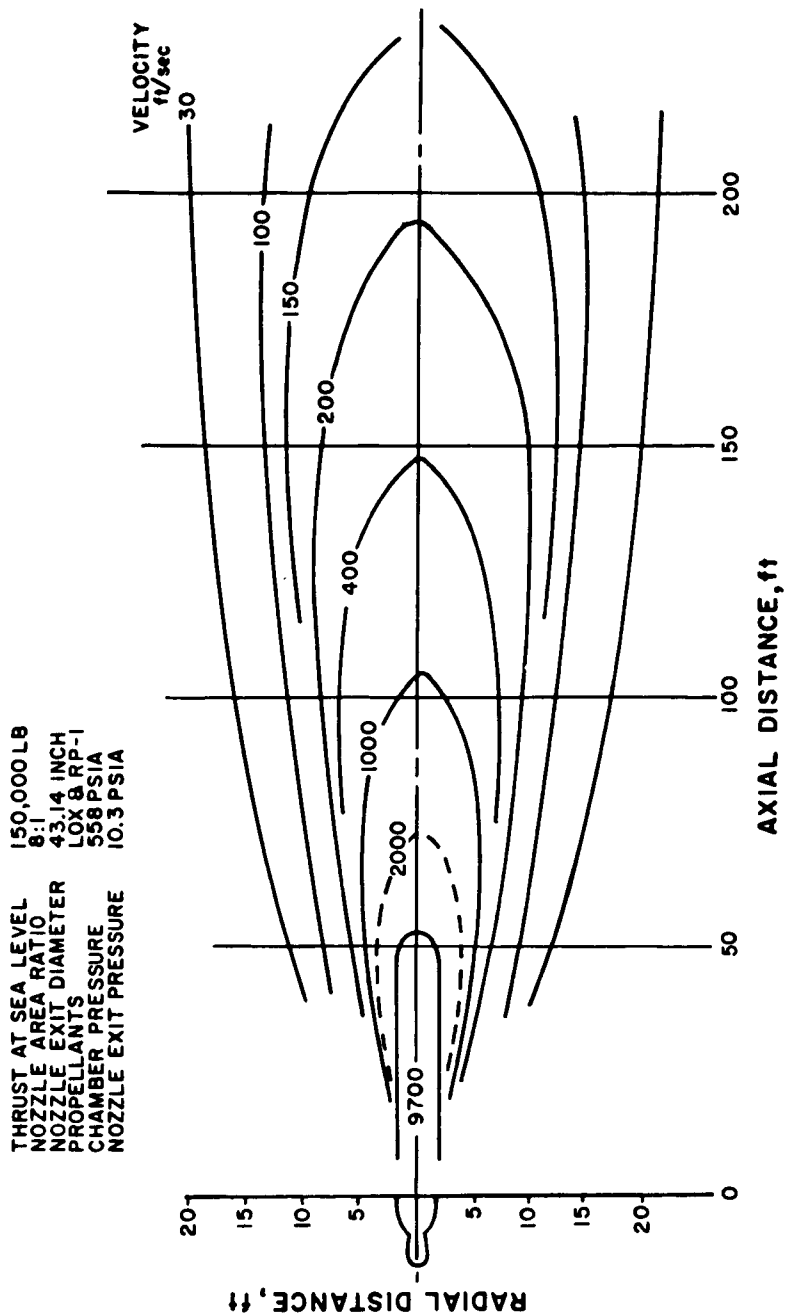


FIGURE 2. VELOCITY DISTRIBUTION IN EXHAUST AT SEA LEVEL OF A 150,000-POUND THRUST ROCKET ENGINE

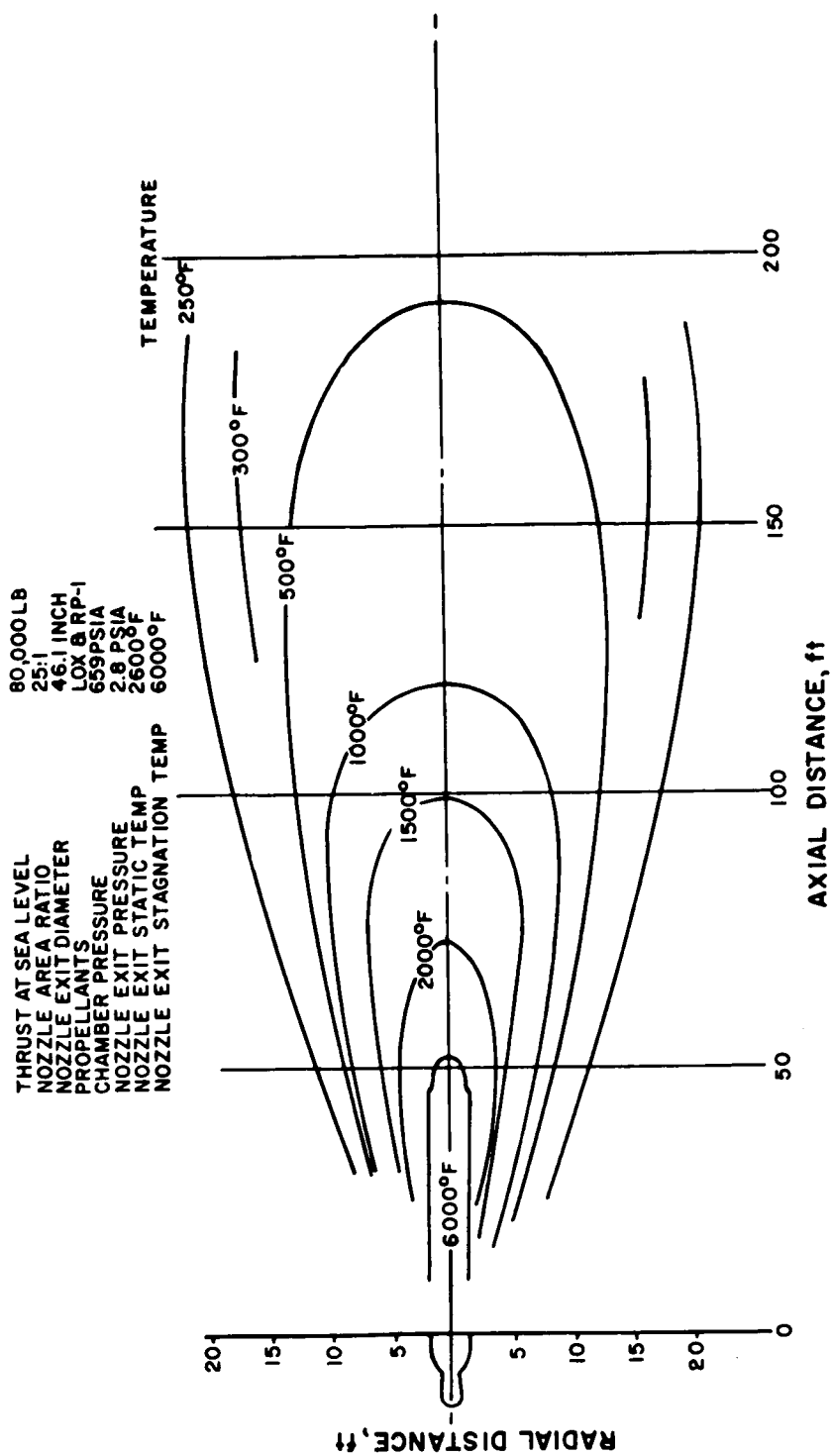


FIGURE 3. TEMPERATURE DISTRIBUTION IN EXHAUST OF AN 80,000-POUND THRUST ROCKET ENGINE

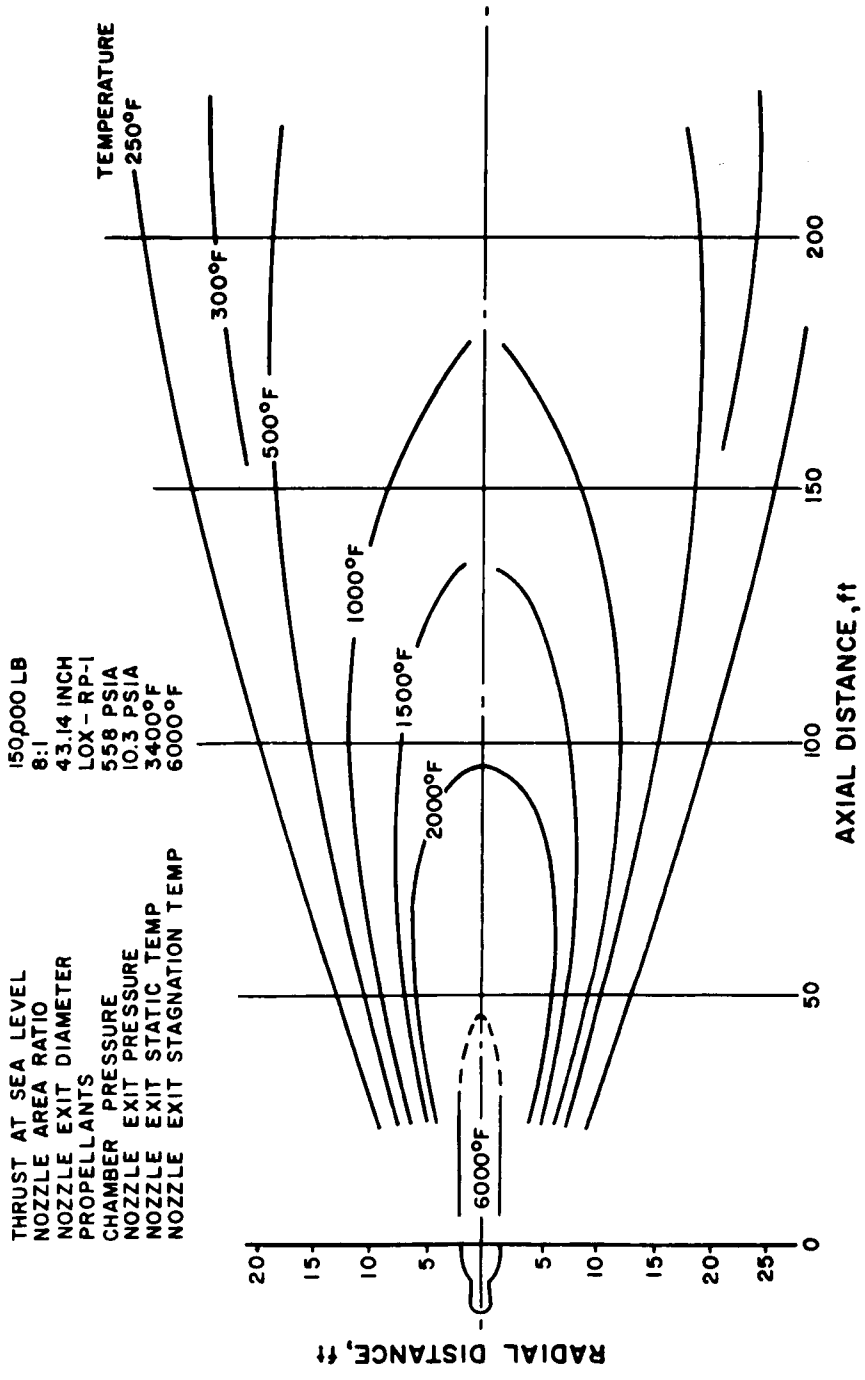


FIGURE 4. TEMPERATURE DISTRIBUTION IN EXHAUST OF A 150,000-POUND THRUST ROCKET ENGINE

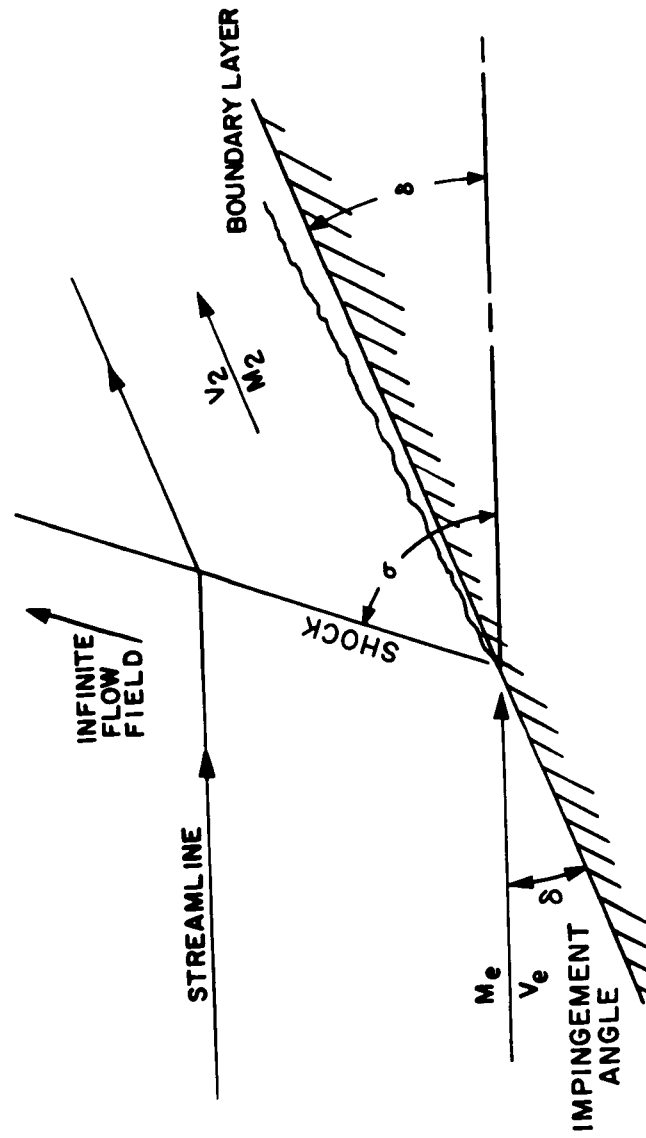


FIGURE 5. JET STREAM IMPINGEMENT OF AN INCLINED PLATE

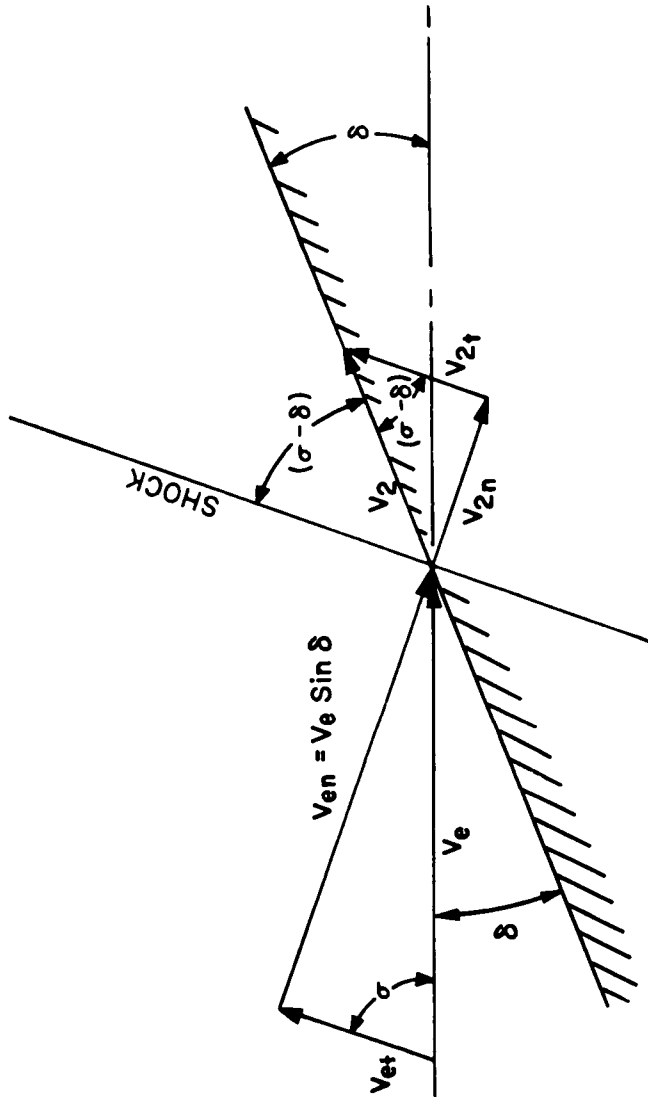
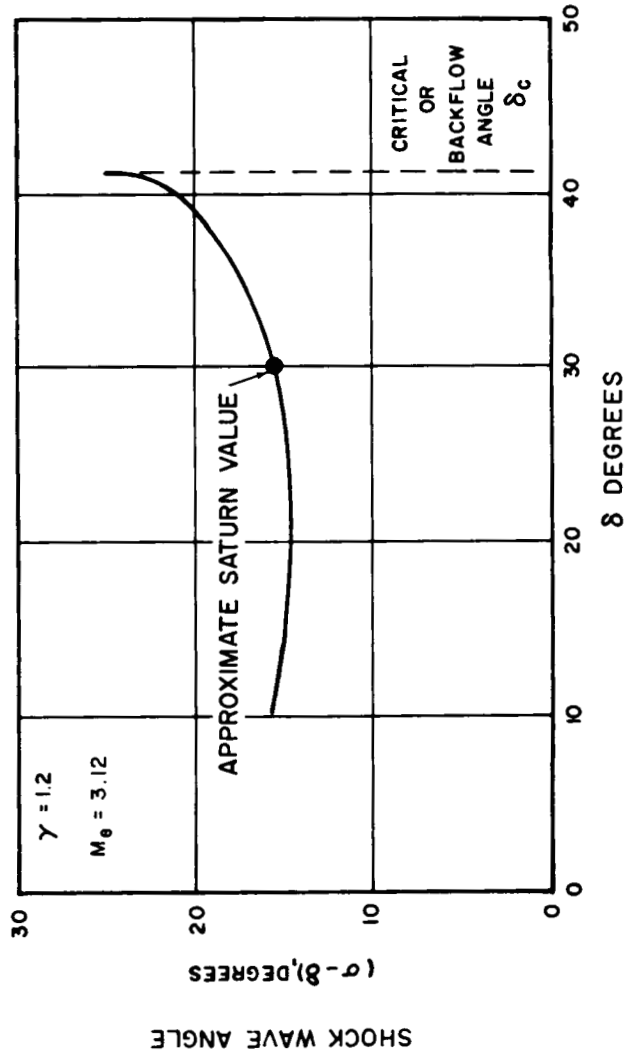


FIGURE 6. VELOCITY VECTOR DIAGRAM OF A JET STREAM IMPINGING ON AN INCLINED PLATE



IMPINGEMENT ANGLE  $\delta$

FIGURE 7. ANGLE WHICH SHOCK WAVE FORMS WITH DEFLECTOR SURFACE VERSUS IMPINGEMENT ANGLE

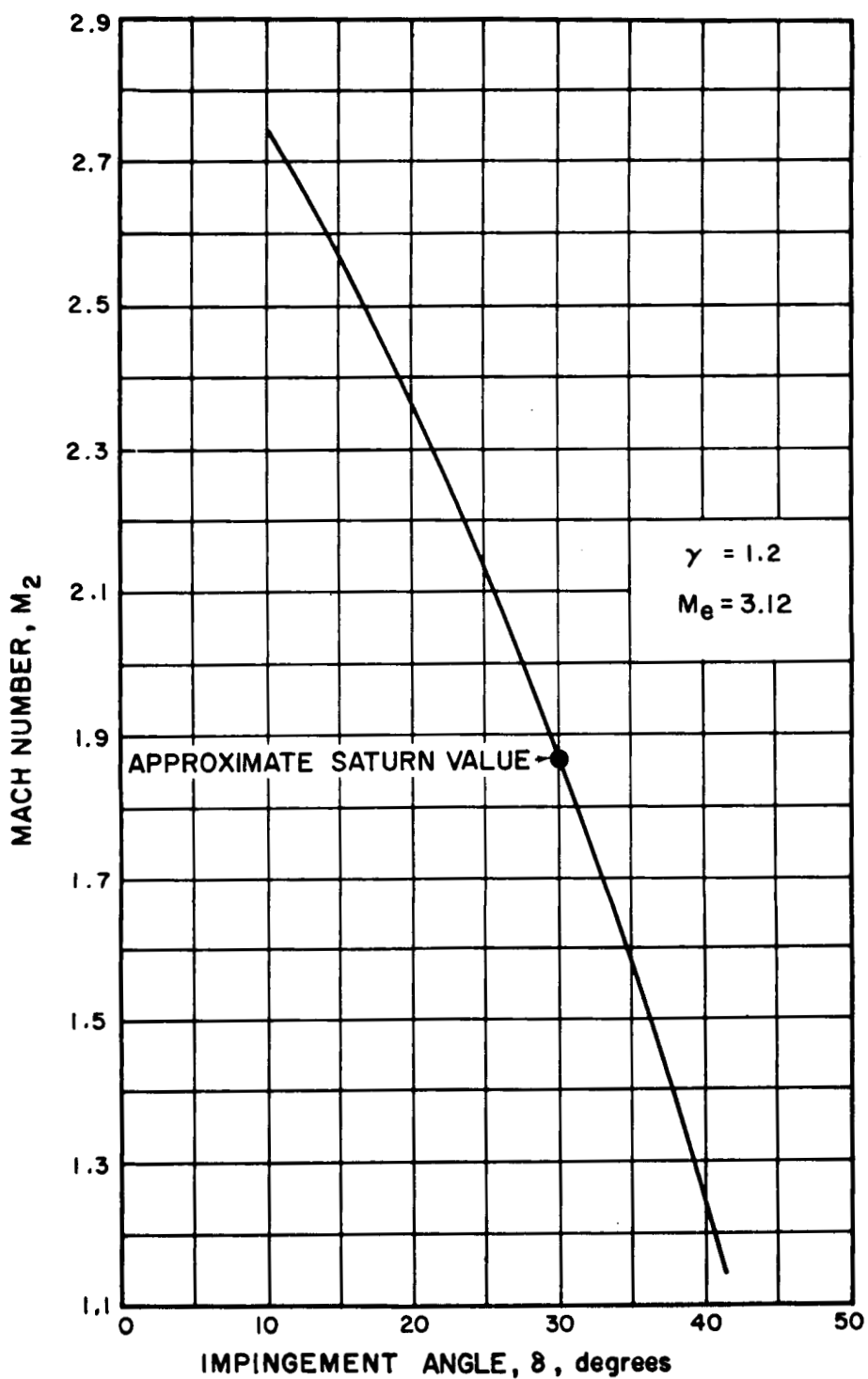


FIGURE 8. MACH NUMBER OF DEFLECTED GAS AFTER PASSING THROUGH AN OBLIQUE SHOCK WAVE VERSUS IMPINGEMENT ANGLE



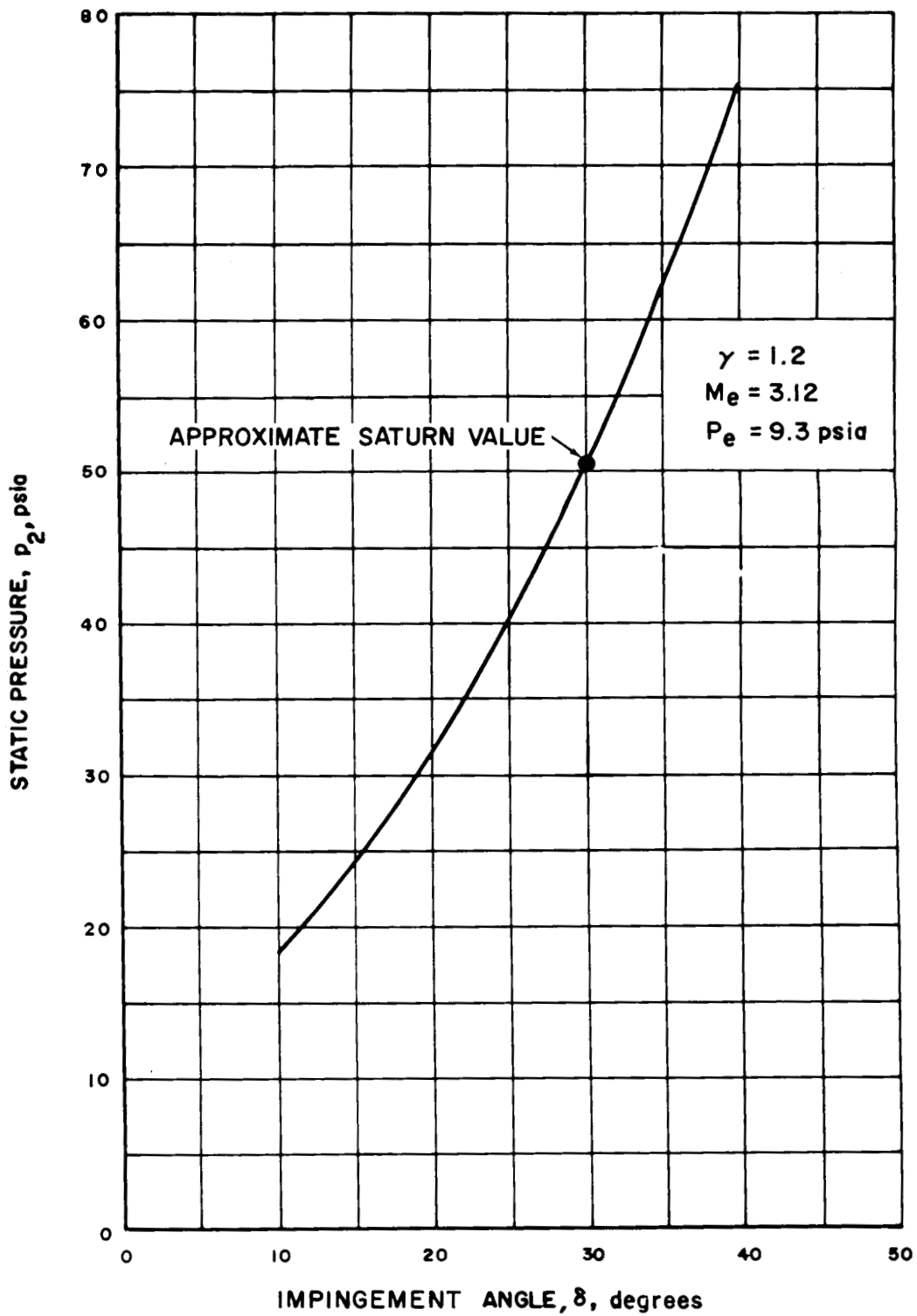


FIGURE 9. STATIC PRESSURE DOWNSTREAM FROM AN OBLIQUE SHOCK WAVE VERSUS IMPINGEMENT ANGLE

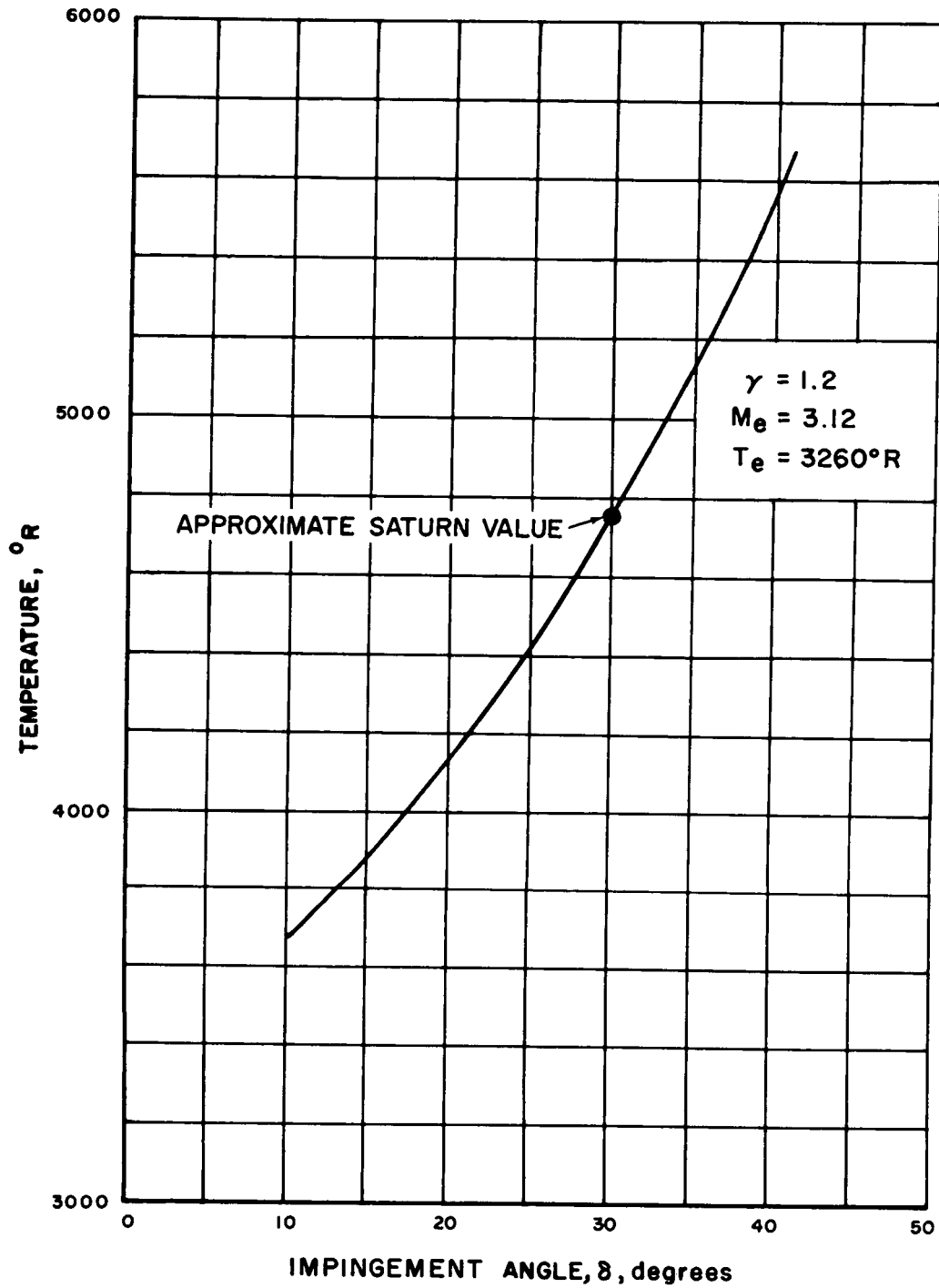


FIGURE 10. STATIC TEMPERATURE OF GAS AFTER PASSING THROUGH AN OBLIQUE SHOCK WAVE VERSUS IMPINGEMENT ANGLE

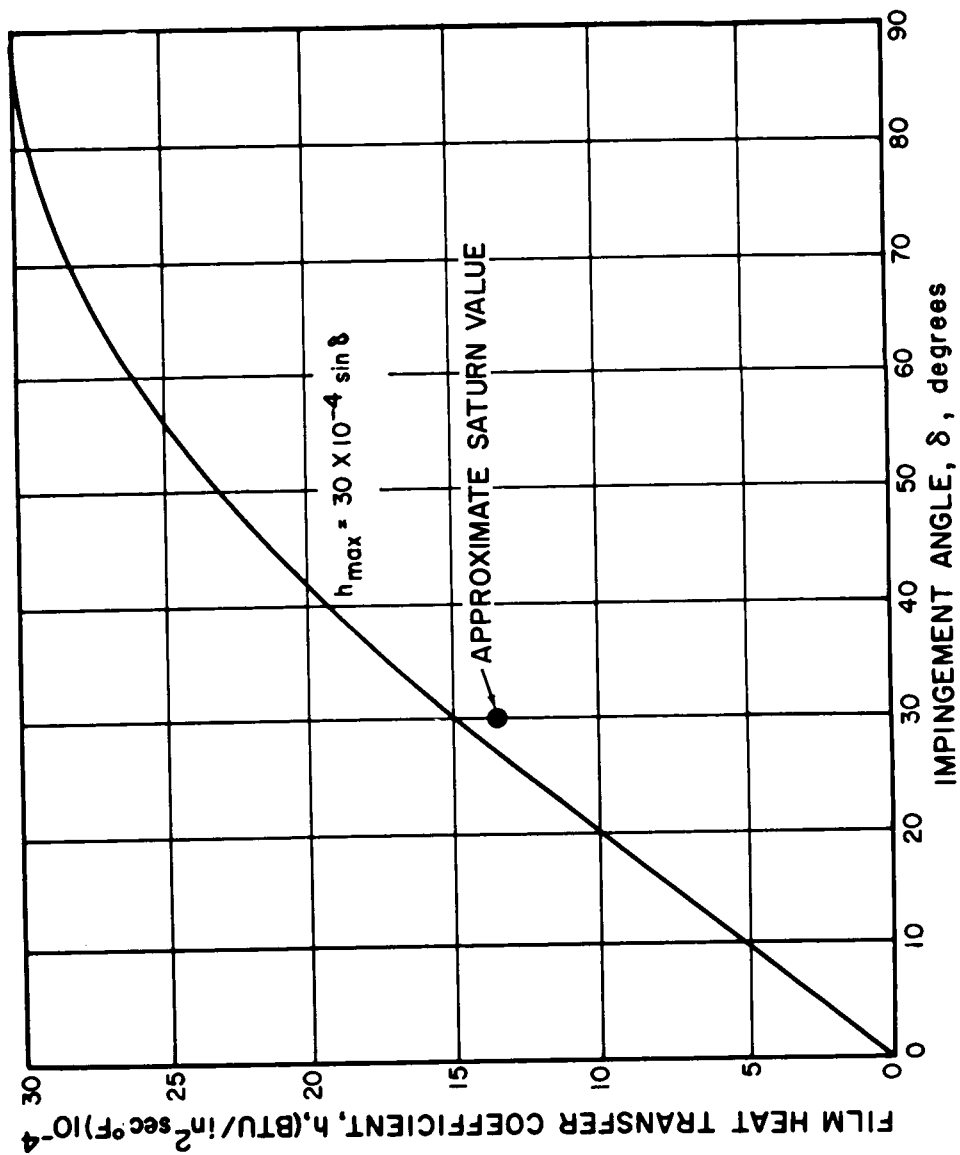


FIGURE 11. FILM HEAT TRANSFER COEFFICIENT VERSUS IMPINGEMENT ANGLE

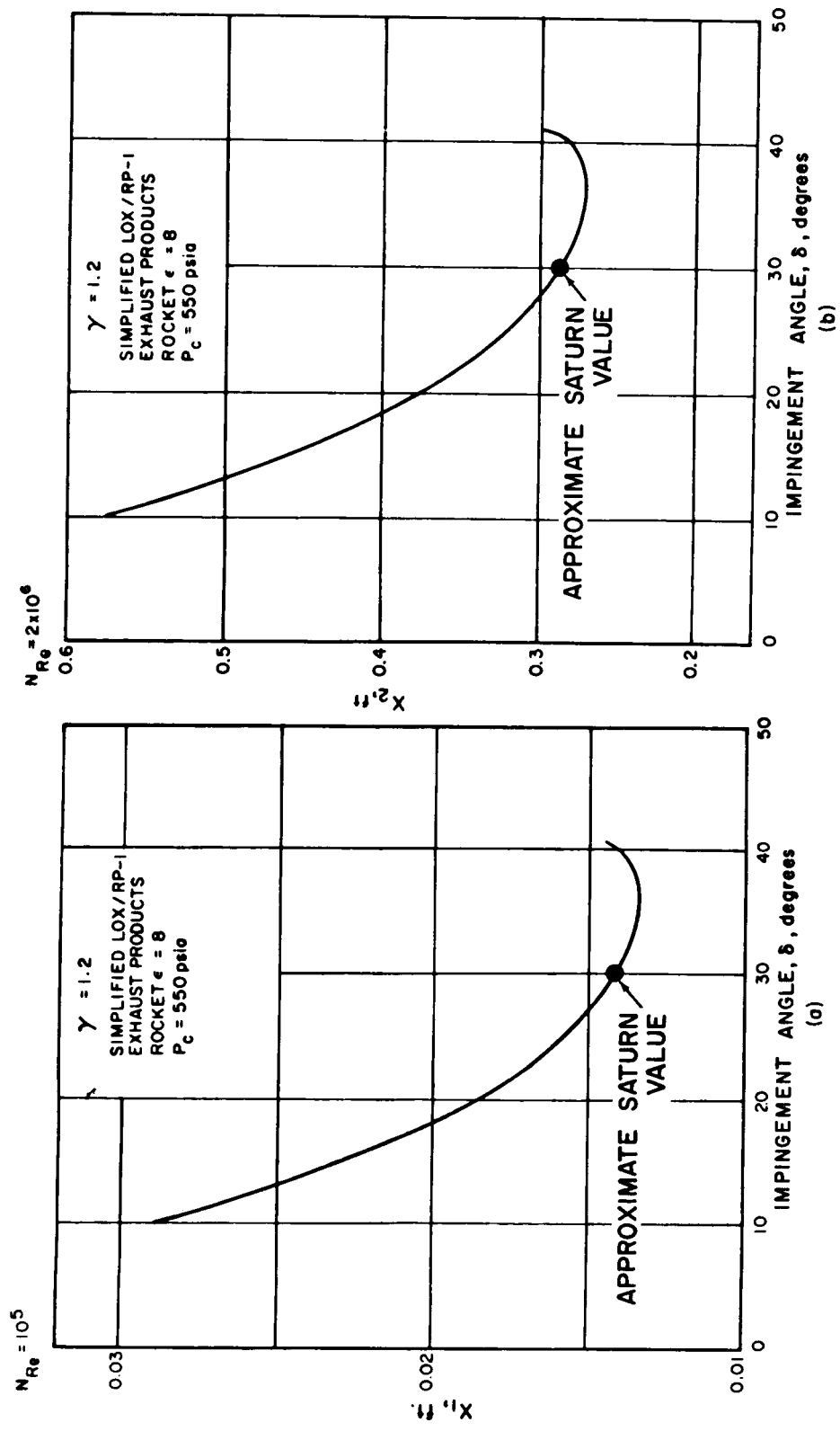


FIGURE 12. DISTANCE FROM FIRST POINT OF IMPINGEMENT TO FULLY DEVELOPED TURBULENT BOUNDARY LAYER FOR TWO DIFFERENT REYNOLDS NUMBERS, VERSUS IMPINGEMENT ANGLE

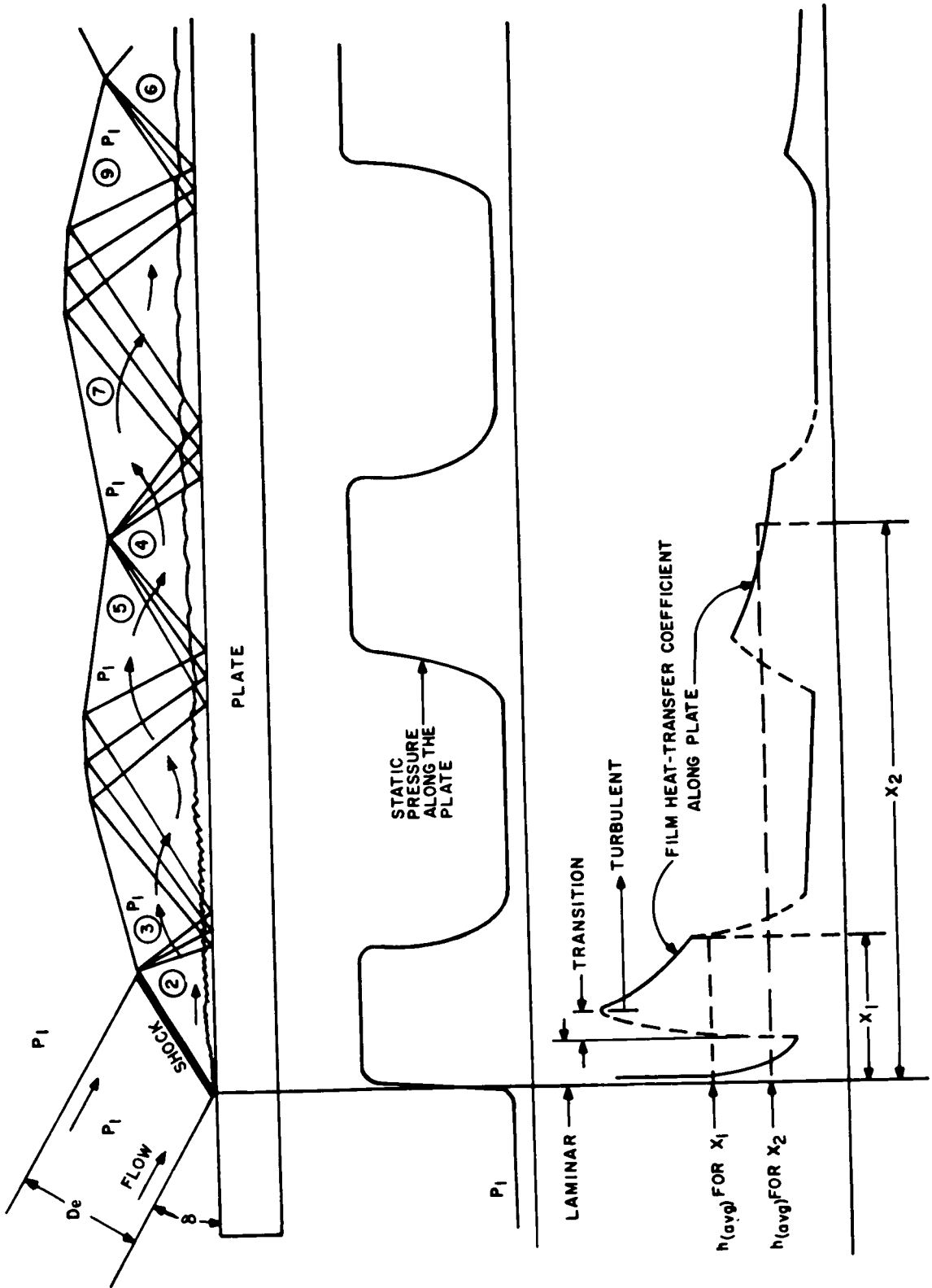


FIGURE 13. FLOW OF A TWO-DIMENSIONAL JET AFTER STRIKING A FLAT PLATE

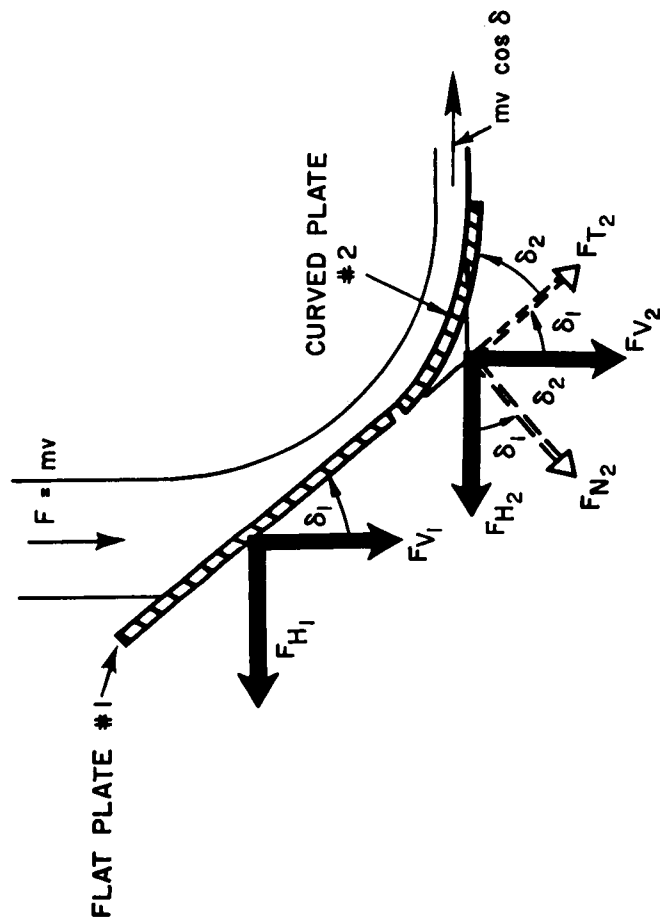


FIGURE 14. FORCES ACTING ON A JET DEFLECTOR UNDER IMPACT OF A SUPERSONIC JET

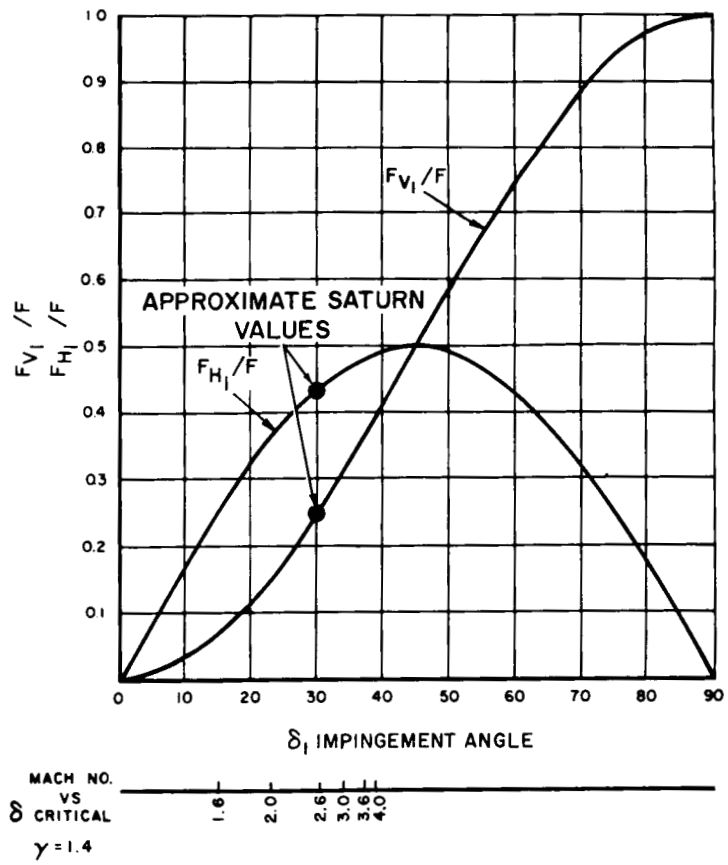


FIGURE 15. COMPONENT FORCES ACTING ON A FLAT PLATE SECTION ORIENTED AT DIFFERENT ANGLES. ALSO MACH NUMBER VERSUS CRITICAL IMPINGEMENT ANGLE

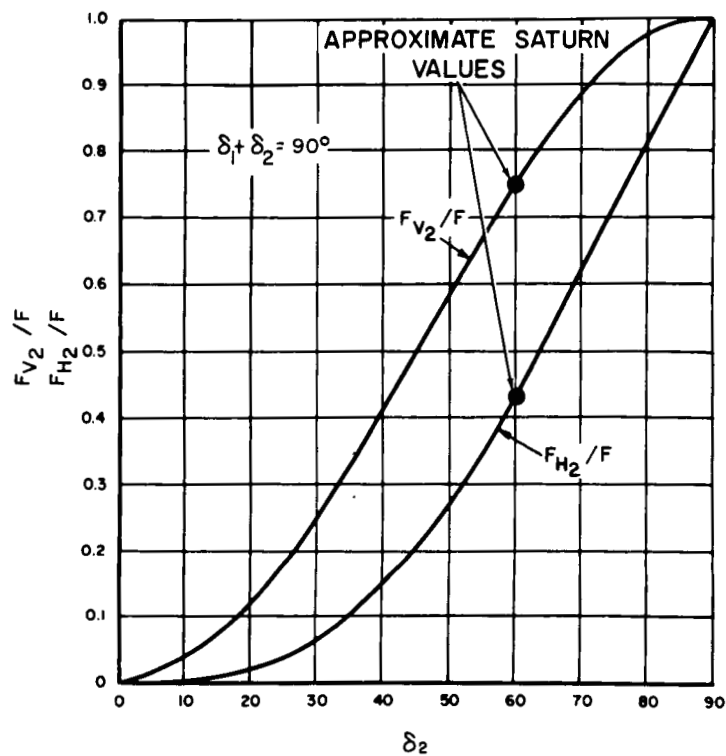


FIGURE 16. COMPONENT FORCES ACTING ON A CURVED PLATE SECTION ORIENTED AT DIFFERENT ANGLES



## ASSUMPTIONS:

- (1)  $h_{\max} = 30 \sin \delta, \text{BTU}/\text{in}^2 \text{ sec } ^\circ\text{F}$
- (2) HEISLER METHOD OF HEAT TRANSFER CALCULATION
- (3) GAS STAGNATION TEMPERATURE  $5000^\circ\text{F}$
- (4) INITIAL WALL TEMPERATURE =  $60^\circ\text{F}$   
(dotted lines indicate data extrapolation)

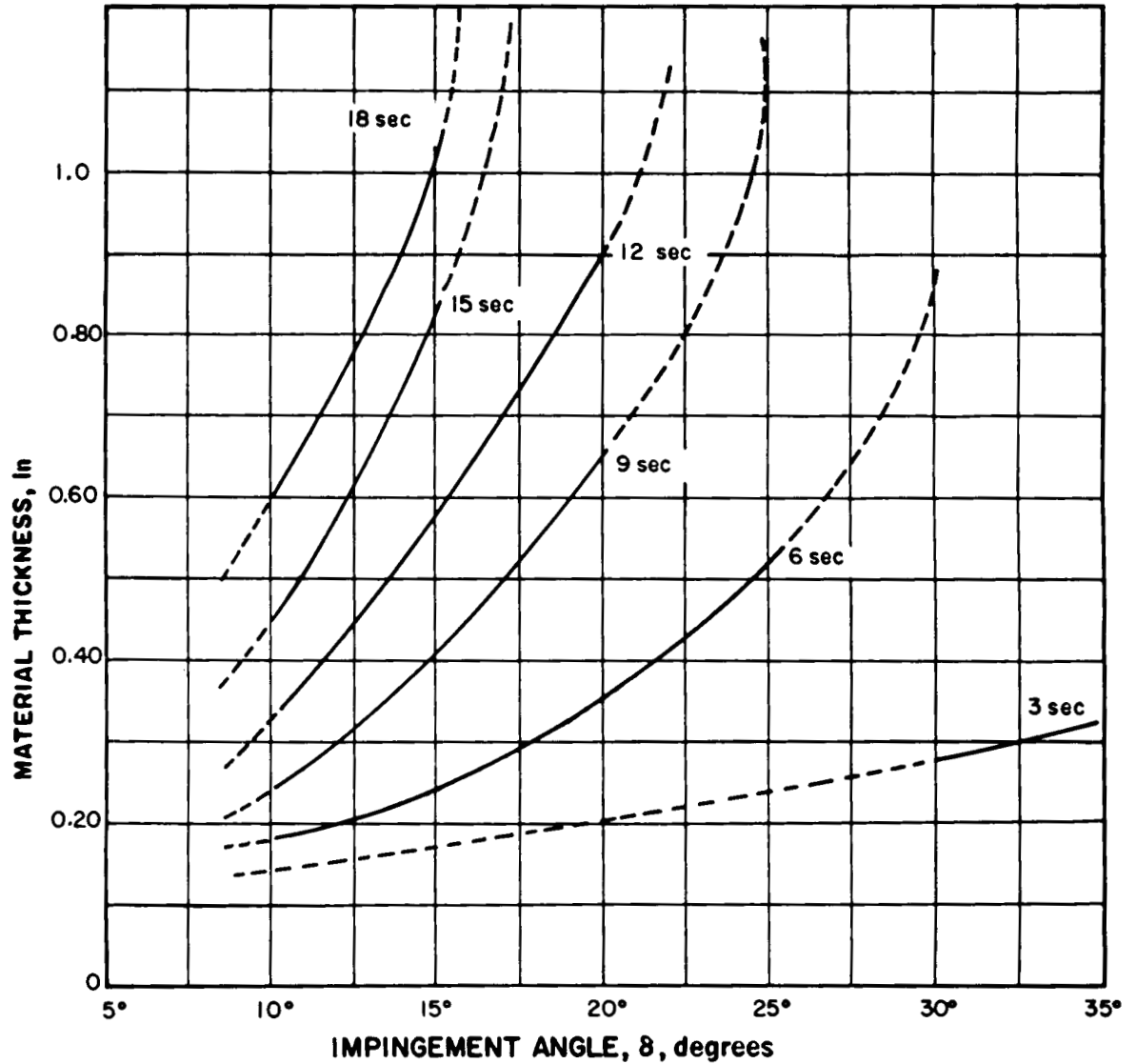


FIGURE 17. STEEL SURFACING THICKNESS VERSUS IMPINGEMENT ANGLE

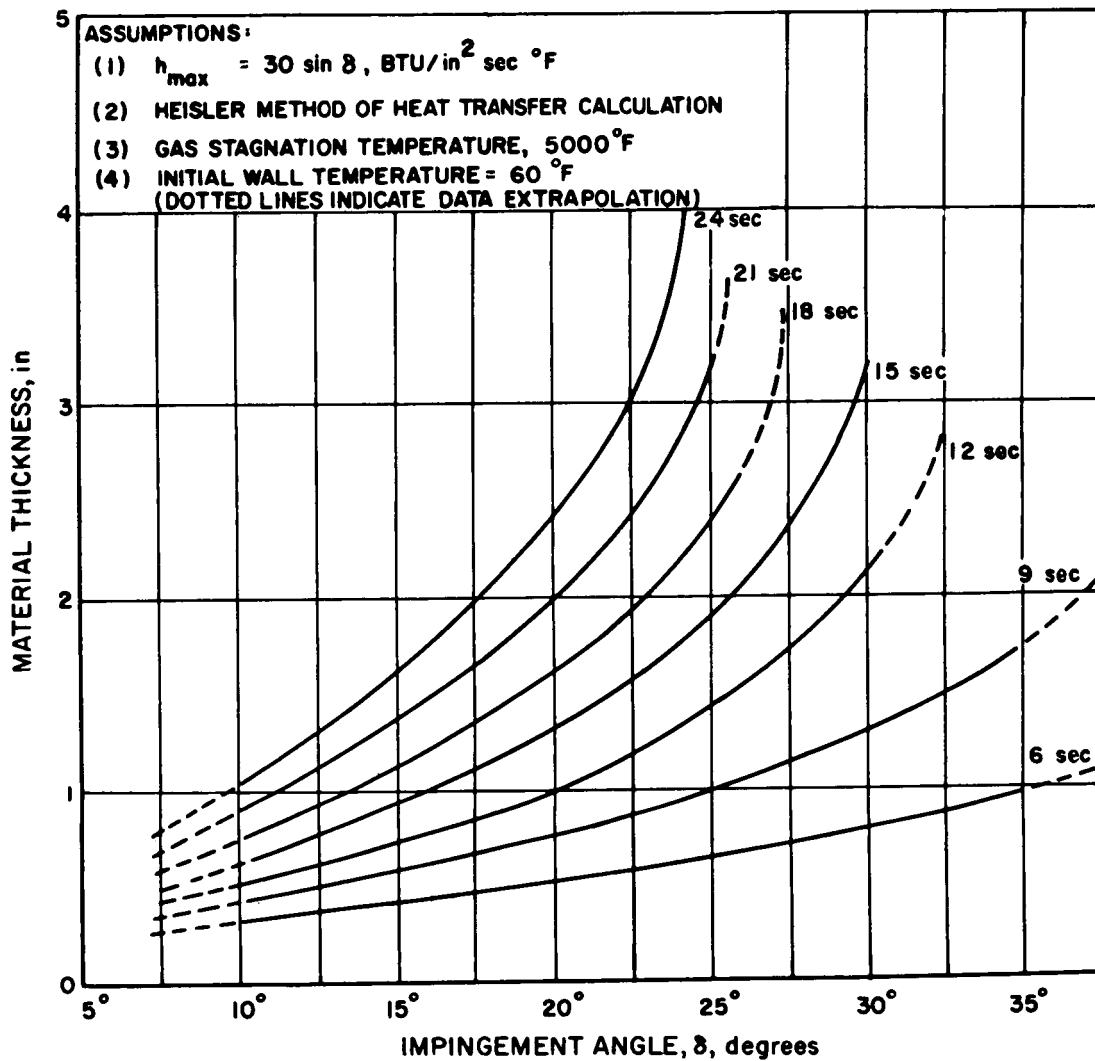


FIGURE 18. COPPER SURFACING THICKNESS VERSUS IMPINGEMENT ANGLE

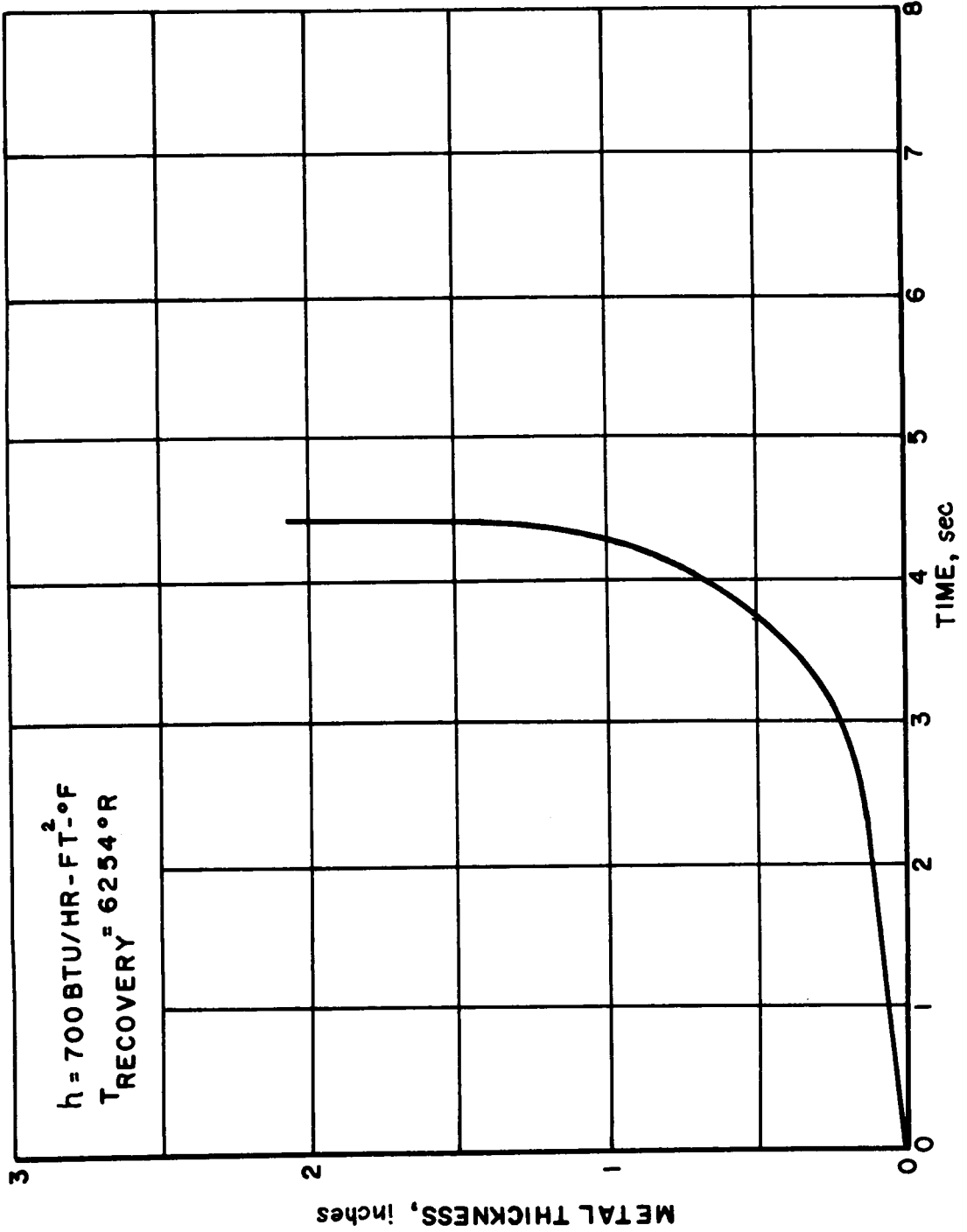


FIGURE 19. TIME REQUIRED FOR EXPOSED SURFACE OF AN INSULATED MILD STEEL PLATE TO REACH A TEMPERATURE APPROXIMATELY 90 PERCENT OF THE MELTING TEMPERATURE AS DETERMINED FROM EXTENDED TRANSIENT HEATING CHARTS

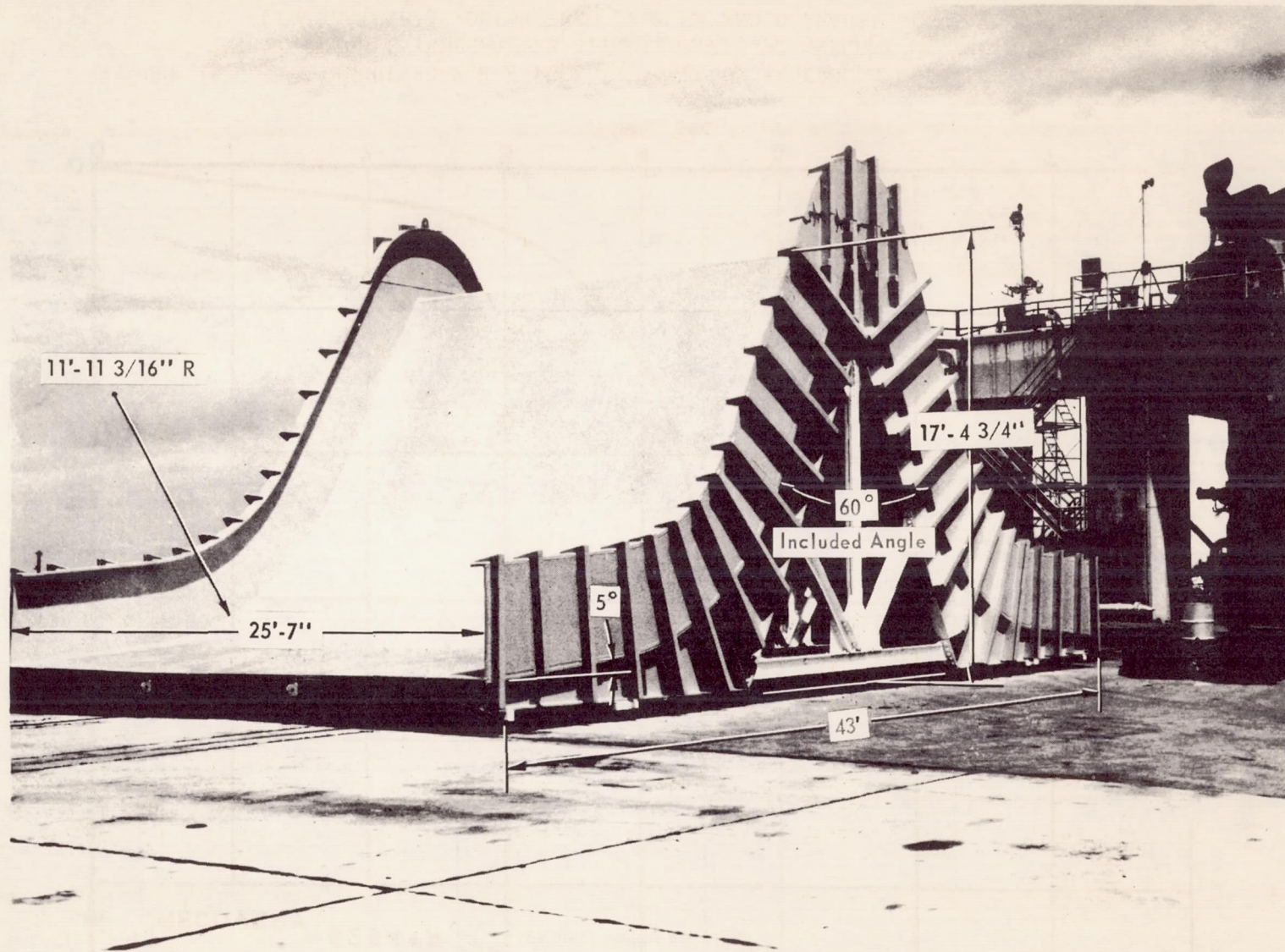


FIGURE 20. SATURN FLAME DEFLECTOR BEFORE VEHICLE LAUNCHING

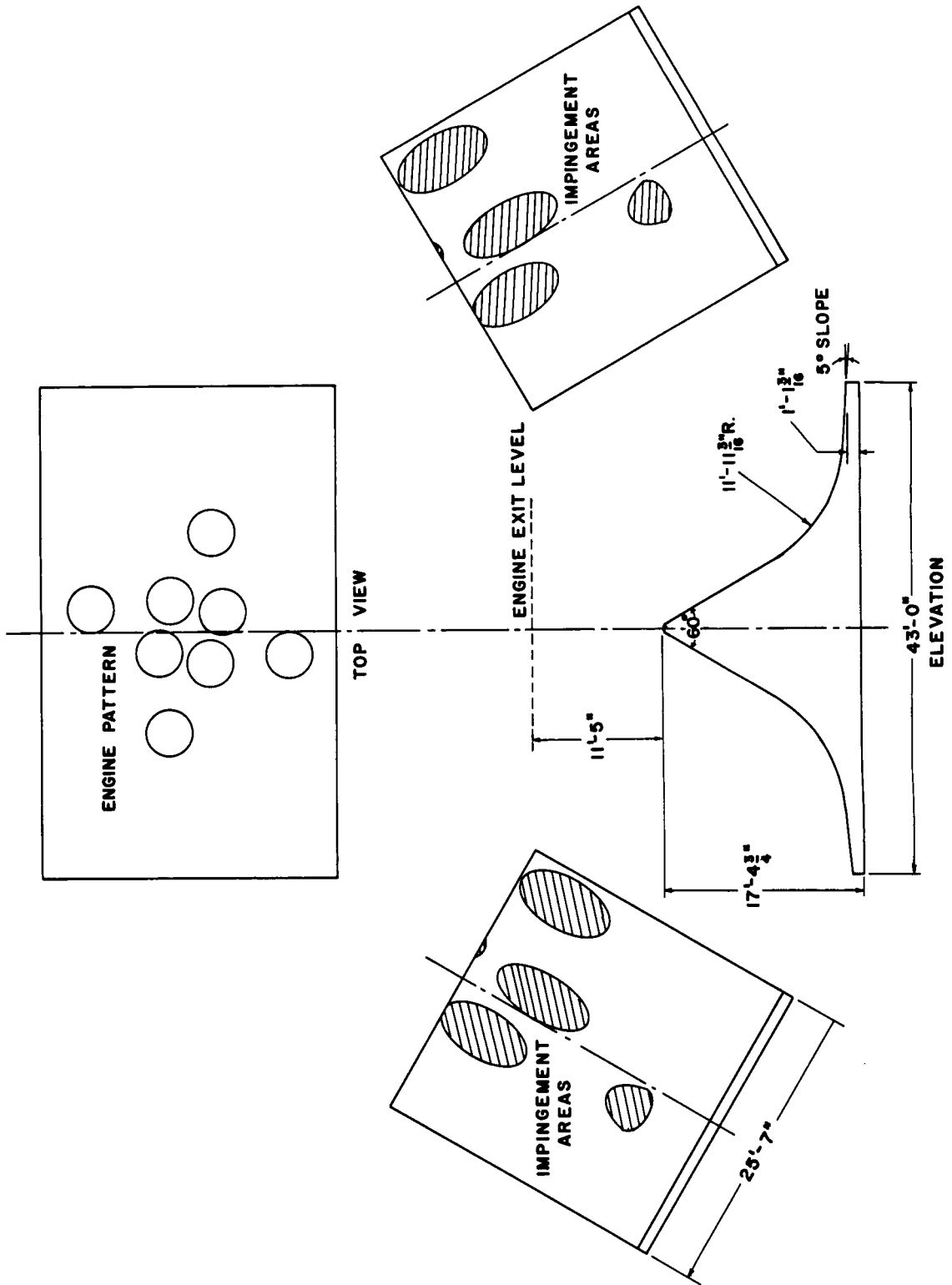


FIGURE 21. FLAME PATTERN ON SATURN DEFLECTOR

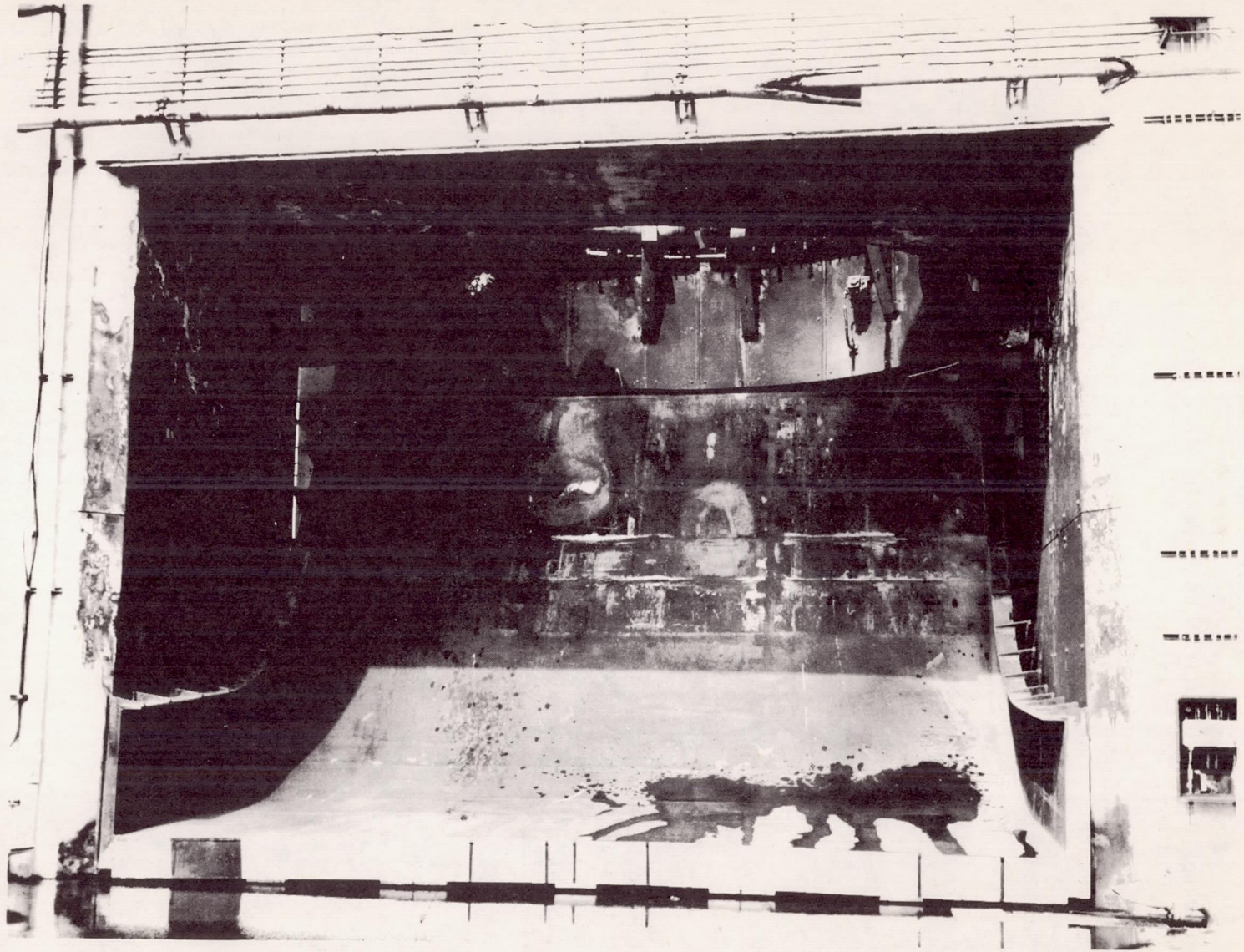


FIGURE 22. SATURN FLAME DEFLECTOR AFTER VEHICLE LAUNCHING

## SPECIFIC REFERENCES

1. Handbook of Astronautical Engineering, H.H. Koelle, McGraw-Hill Book Company, Inc., 1961.
2. On Uncooled Flame Deflectors for Rocket Propelled Missiles, by A.N. Baxter, USAF, GM-TR-0165-00332, February 17, 1958.
3. The Dynamics and Thermodynamics of Compressible Fluid Flow, A.H. Shapiro, Ronald Press Company, 1953, Volume I.
4. Design Information for Uncooled Flame Deflectors, Aerojet General, Corp. (Confidential), USAF 04(647)-81 Part II Item 5C.
5. On The Extension of Transient-Heating Charts For The Semi Infinite Slab, A.N. Baxter STL/TN-59-0000-09355, 15 December 1959.

## GENERAL REFERENCES

1. Design Criteria for Launchers and Deflectors prepared for Army Ballistic Missile Agency by Vitro Engineering Company under the direction of the Mechanical Branch of the System Support Equipment Laboratory, ABMA, Contract No. DA-30-069-ORD-2331, March 10, 1960.  
CONFIDENTIAL